DESIGN OPTIMIZATION OF AN X-BAND BASED FEL

A. Aksoy*, Ankara University, Ankara, Turkey
A. Latina, J. Pfingstner, D. Schulte, CERN, Geneva, Switzerland
Z. Nergiz, Niğde University, Niğde, Turkey

Abstract

A design effort for a new generation of compact, cost-effective, power-efficient FEL facilities, based on X-band technology, has been launched. High-frequency X-band acceleration implies strong wakefields, tight alignment and mechanical tolerances, and challenging stability issues. In this paper a design is proposed for the injector and the linacs, including the two bunch compressors. RF gun and injector simulations have been performed, successfully meeting the stringent requirements in terms of minimum projected emittance, sliced emittance and minimum bunch length. In the design of the linac and bunch compressors wakefield effects and misalignment have been taken into account. Start-to-end tracking simulations through the optimized lattice are presented and discussed.

INTRODUCTION

The high accelerating gradients achievable with X-band structures allow the design of shorter and more power-efficient linacs than S-band and C-band ones, extending the energy reach and opening up the way to a next generation of light sources and linear colliders. The encouraging development of power sources for X-band structures [1] gives this technology the opportunity to be used in general-purpose accelerators. Besides, recent studies of operating CLIC X-band accelerating structures at gradients higher than 100 MV/m with low RF breakdown rate [2] confirmed the potential for the X-band technology to provide an effective solution to get very compact and cost-effective multi-GeV linacs, for example FELs. Taking advantage of the advancements in the X-Band technology, a group of 12 institutions and universities have RF a collaboration to exploit CLIC-like X-band accelerating structures to drive a greenfield FEL facility [3]. Due to the small volume, the efficient RF operation, the reduced cooling requirements, the possibility of operation at higher repetition rates than S/C band structures (e.g. up to 500 Hz), X-band-based FELs will create new research areas for FEL physics and applications. In this paper, we describe the design an according simulation studies of an "all X-band" XFEL (including the gun), operating at a acceleration frequency of 12 GHz.

MACHINE DESCRIPTION

The proposed facility has of an X-band based injector followed by a a two-stage 6 GeV linac, which can deliver a high-repetition, low-emittance beam. This beam is fed into the undulator sections and the created X-rays are guided via photon lines for the user stations. The proposed layout is shown with Fig. 1. The expected length of the facility is about 550 m, and its basic parameters are given in Table 1.

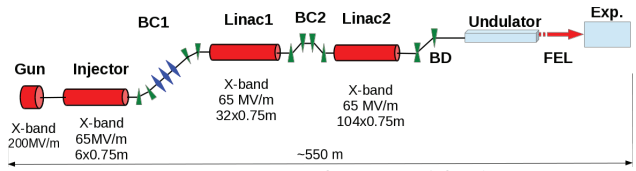

Figure 1: Layout of proposed facility.

Table 1: Parameters of an X-band Linac Based X-FEL Facility

Parameter	Unit	Value
Energy	GeV	6
Bunch Charge	pC	250
Normalized emittance	μmrad	<0.5
RMS Bunch Length	μm	9
Linac frequency	GHz	12
RF pulse length at structure	ns	150
Pulse repetition rate	Hz	50-500
Number of bunches per pulse	#	1-3
No of structures per RF module	#	8
Total (effective) module length	m	9.8 (6.16)
Number of RF modules needed	#	17.5
Linac gradient	MV/m	65
No of klystrons per RF module	#	2
Klystron output power	MW	50
Klystron output pulse length	μs	1.5
Total (effective) linac length	m	250 (107.5)

Injector

The injector is proposed to be the similar to the X-band RF photo-cathode gun set up being developed at SLAC [4]. The injector starts with 5.6 cell photocathode gun operating at 12 GHz with peak accelerating voltage of 200 MV. This is followed by 6 traveling-wave accelerating structures operating at 12 GHz with 65 MV/m gradient and 150° phase advance per cell, which accelerate the beam to 300 MeV. The layout of injector is given with Fig. 2.

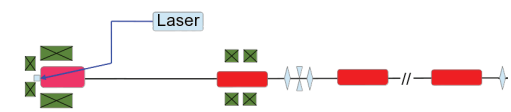

Figure 2: Layout of the proposed injector.

* avniaksoy@ankara.edu.tr

ISBN 978-3-95450-147-2

After designing preliminarily the RF gun and solenoids using Poisson/Superfish code [5] beam dynamics studies in the injector have been performed using the ASTRA code [6]. The length of the first half cell, position of the first accelerating structure, the strength of the solenoids and the phase of RF structures are optimized to provide minimum sliced and projected emittance. Fig. 3 shows the results along the gun and the first accelerating structure of injector. In simulation a flat top laser pulse with length of 3 ps has been assumed.

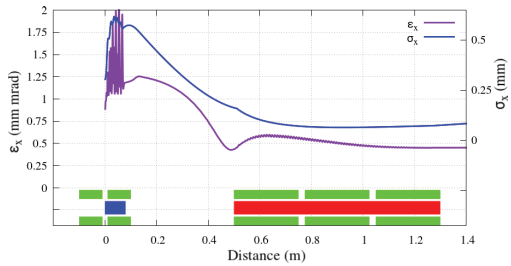

Figure 3: Beam envelope and beam size variation along the gun and the first accelerating structure of the injector.

Pulse Compressor and RF Module Layout

In order to establish the optimal number of structures per module, we considered the impact of single-bunch wake field effect along the main linac. As the beam travels through the linac, the bunch head undergoes an unperturbed transverse motion, whereas the tail experience due to the wakefields excited by the leading particles. In normalized transverse coordinates, the amplitude of the deflection is amplified by a factor A,

$$A = \frac{Ne^2}{2} \int_0^L \frac{\beta(s)}{E(s)} V_\perp(s) ds \qquad (1)$$

where N is number of particles per bunch, β is beta function along the linac, E is energy, and $V_\perp$ is the transverse wake potential of the structures [7], which is given by

$$V_{\perp,\parallel}(s) = \int_{-\infty}^{s} ds' \lambda(s') W_{\perp,\parallel}(s - s'), \qquad (2)$$

where λ is the longitudinal charge distribution and $W_{\perp,\parallel}$ is transverse,longitudinal wake function of structure [8]. In order to optimize the number of structure per module we have used a FODO-type lattice and to calculated A_{max} along linac 1 for different charge distributions, bunch lengths and numbers of structures per module. The result is depicted in Fig. 4, where an uniform longitudinal charge distribution has been assumed. As can be seen, the amplification decreases with shorter bunch length. The acceptable amplification factor has been chosen to be below 2. Therefore, one should use a maximum of 8 structures on the module which and the bunch length should be below 80 μm in linac 1.

Hence, 8 structures will be mounted on one RF module, which is fed by one RF station. The station may consist of several klystrons to provide sufficient power [9]. We assume that a single 100 MW RF pulse of 1.5μs length is

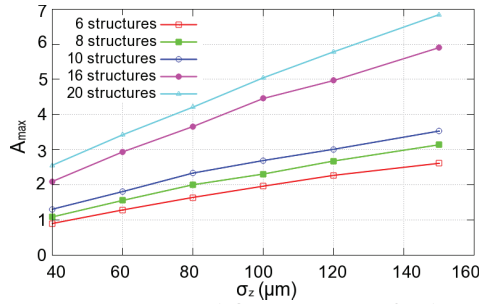

Figure 4: Maximum amplification A_{max} for linac 1 as a function of bunch length for different numbers of structures per module.

be compressed to 150 ns using a SLED-II pulse compressor [10]. After compression, the expected RF power is 468 MW. The compressed power will be evenly distributed by an RF network to each structure, feeding each structure with about 50 MW, which corresponds to a gradient of 70 MV/m.

Magnetic Bunch Compressors

We have designed a dogleg-type bunch compressor similar as proposed in [11], in which the bunches are almost linearized by optical elements located in first bunch compressor. This approach suits X-band acceleration, because it's harder to find and operate high-harmonic RF structures, i.e., above 30 GHz. In order to achieve a large compression factor in short distance a pair of bending magnets each bending by 5.5° have been used. Quadrupoles and sextupoles are used in such a way that second order longitudinal dispersion of BC1 cancels the second order energy correlation in the electron beam and obtain achromaticity. Figure 5 shows the Twiss Functions along the first bunch compressor.

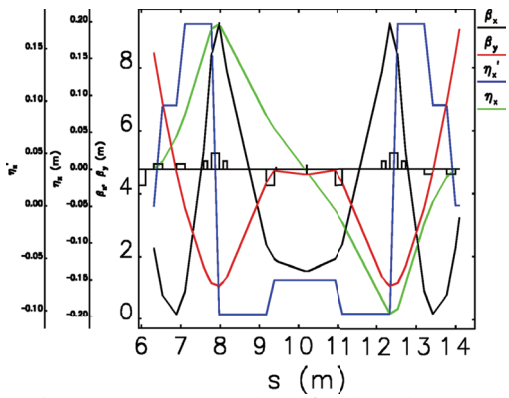

Figure 5: Twiss Functions along first bunch compressor.

The second bunch compressor has been chosen to be a chicane, featuring four dipole magnets with bending angle 2.2°. The full compression has been optimized by considering both compressors, injector linac and linac 1.

SIMULATIONS

Full 6-D Tracking simulations have been performed using both Placet [12] and Elegant [13] codes. The simulation of starts at a beam energy of 60 MeV using the distribution

created by the ASTRA code and tracks this distribution through the full lattice including the bunch compressors. The start-to-end first order optics is illustrated in Figure 6.

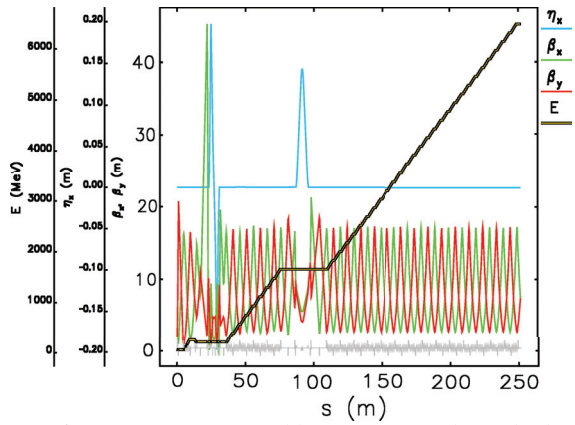

Figure 6: Beta Functions and beam energy along the linac.

The final bunch distribution and its parameters are shown in Figure 7. As it is seen, the bunch is compressed to a length 9 μm with an RMS energy spread of 0.03% at the end of the linac, which is acceptable for the lasing process.

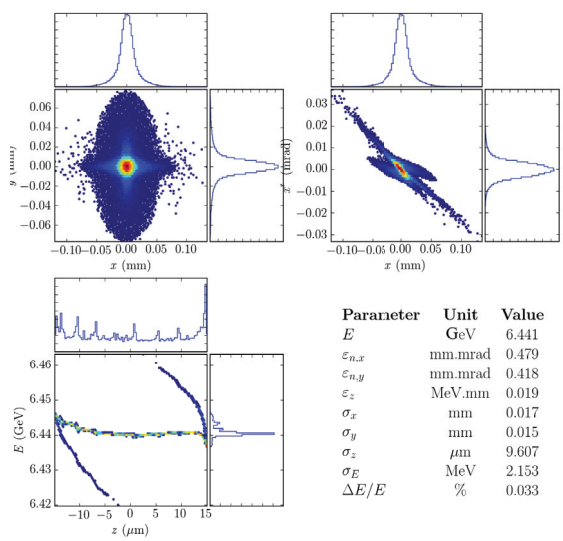

Parameter	Unit	Value
E	GeV	6.441
$\varepsilon_{n,x}$	mm.mrad	0.479
$\varepsilon_{n,y}$	mm.mrad	0.418
ε_z	MeV.mm	0.019
σ_x	mm	0.017
σ_y	mm	0.015
σ_z	μm	9.607
σ_E	MeV	2.153
$\Delta E/E$	%	0.033

Figure 7: Parameters, phase spaces and transverse distribution of the beam at the end of linac with associated histograms.

The growth of emittance due to static alignment errors have also been simulated with three different beam-based alignment methods; one-to-one correction, Dispersion-Free Steering and Wakefield-Free Steering. In simulations all elements are scattered transversely with 100 μm offset from their ideal position. In addition the dipoles and RF structures are assumed to have 100 μrad angle errors. The simulations have been averaged over 100 simulated machines and each machine is corrected with correctors and BPMs that have resolution of a 5 μm. The result is shown in figure 8. The tests confirm that the final emittance can be kept below 0.5 $\mu mrad$ in both axes.

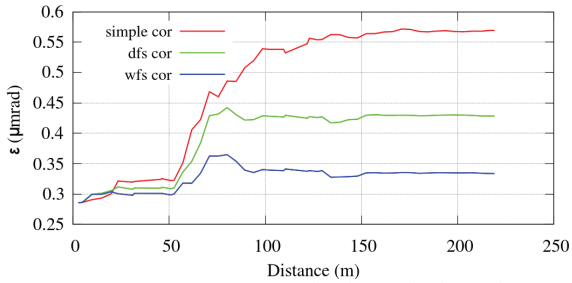

Figure 8: Emittance growth along the beamline.

We have also performed simulations of the lasing section using GENESIS [14] code. We have used planar undulators and a quadrupole FODO lattice. We assumed each undulator is about 4.2 m long, with 15 mm period and undulator strength $K_{RMS} = 1$. Using the longitudinal bunch distribution given with Fig. 7 we find that the power of laser at 0.9 resonant wavelength saturates at around 30 m and power reaches to 5 GW in SASE operation which is typical number for X-FELs. Fig. 9 shows the temporal FEL power at the undulator exit.

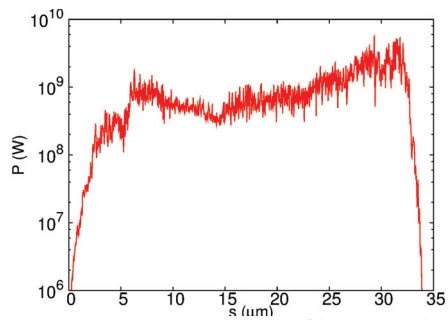

Figure 9: FEL power temporal profile at undulator exit.

CONCLUSION

In this paper, we present the design of an "all X-band" hard X-ray FEL facility. The design includes a photo-cathode RF gun and a two-stage 6 GeV linac, both utilising X-band technology. The bunch is compressed via a two-stage system to reach a peak current of 3 kA. The first bunch compressor uses optical linearisation to avoid the need of higher-harmonic RF for the phase space linearization. FEL simulations indicate that lasing at 0.9 wavelength is possible in an undulator with period length 15 mm and strength K_{RMS} of 1. The proposed FEL saturates below 30 meters, with an average generated power of about 5 GW. In future work, we plan to evaluate the emittance growth induced by ISR, CSR, wakefields, small variations in acceleration phase and voltage, magnetic field errors and injection timing jitter. For the undulator sections, self-seeding and tapering will be simulated as well as the effect of transverse beam jitter and size oscillations on the FEL performance.

ACKNOWLEDGEMENT

The authors would like to thank W. Wuensch and I. Syratchev for their assistance with X-band technology.

ISBN 978-3-95450-147-2

REFERENCES

[1] J. Kovermann et al., "Commissioning of the First Klystron-Based X-band Power Source at CERN", Proceedings of IPAC2012, New Orleans, Louisiana, USA, paper THPPC060, pp. 3428-3430 (2012).

[2] A. Degiovanni et al., "High-gradient test results from a CLIC prototype accelerating structure: TD26CC", Proceedings of IPAC2014, Dresden, Germany, paper WEPME015, pp. 2285-2287 (2014).

[3] J. Pfingstneret et al., "The X-Band FEL Collaboration", Proceedings of FEL2015, Daejeon, Republic of Korea, paper TUP013, pp. 368-374 (2015).

[4] R. A. Marsh et al., "Modeling and Design of an X-band RF Photoinjector", Phys. Rev. ST Accel. Beams, v. 15, p. 102001, (2012).

[5] James H. Billen, "POISSON/SUPERFISH user's Manual", LA-UR-96-1834 , LANL, (2006).

[6] K. Floettmann, "ASTRA User Manual", DESY, (2011).

[7] A. Aksoy, et al., "Beam dynamics simulation for the Compact Linear Collider drive-beam accelerator", Phys. Rev. ST Accel. Beams, v. 14, i. 8, p. 84402, (2011).

[8] K. Bane, SLAC Report No. SLAC-PUB-9663, (2003).

[9] A. Aksoy et al., "Conceptual Design of an X-FEL Facility Using CLIC X-Band Accelerating Structure" , Proceedings of IPAC2014, Dresden, Germany, paper THPRO025, pp. 2914-2917, (2014).

[10] C. Hantista et al., "High-power RF pulse compression with SLED-II at SLAC," Proceedings of Particle Accelerator Conference, Washington, DC, USA, pp. 1196-1198, vol. 2, (1993).

[11] Y. Sun, et al., "X-band RF Driven Free Electron Easer Driver With Optics Linearization", Phys. Rev. ST Accel. Beams 17, 110703 (2014).

[12] D. Schulte et al., The PLACET Tracking Code, `http://clicsw.web.cern.ch/clicsw/`

[13] M. Borland, "User's Manual for Elegant", (2013).

[14] S. Reiche, GENESIS 1.3, `http://genesis.web.psi.ch`